Nuclear Multicatalytic Proteinase Subunit RRC3 Is Important for Growth Regulation in Hepatocytes†

Catharine M. Benedict and Gary A. Clawson*

Departments of Pathology, Biochemistry and Molecular Biology, and Cell and Molecular Biology Program, The Pennsylvania State University, Hershey, Pennsylvania 17033

Received April 12, 1996; Revised Manuscript Received June 28, 1996⊗

ABSTRACT: Multicatalytic proteinases (MCPs) are macromolecular structures involved in the intracellular degradation of many types of proteins. MCPs are composed of a 20S "core" of both structural (α) and presumed catalytic (β) subunits, in association with regulatory proteins. They are characteristically found in both the nucleus and cytoplasm of cells, although mechanisms governing the subcellular distribution of MCPs are not known. RRC3, an α subunit of rat MCPs, contains both a putative nuclear localization signal (NLS) and a potential tyrosine phosphorylation site which could play a role in nuclear import, and the nuclear form of RRC3 appears to be involved in the regulation of cell growth. Here we have generated a variety of RRC3 expression constructs to study features of RRC3 important in nuclear localization and cell growth. PCR was utilized to develop constructs containing point mutations in either the putative NLS (K_{51} mutated to A) or at a potential tyrosine phosphorylation site (Y_{121} mutated to F), and an epitope from influenza hemagglutinin (HA) was added in triplicate to the C-terminus of the constructs as a means of identification. RRC3 constructs were then made in which the nucleotide sequence near the translation initiation site of RRC3 was modified in such a way that the amino acid sequence of the protein translated from the constructs is unchanged from that of normal RRC3, thus allowing differential modulation of endogenous RRC3 with antisense oligonucleotide treatment. These N-terminally modified constructs are designated mC3, $mC3_{NLS}$, and $mC3_Y$. *In vitro* transcription/translation reactions with these constructs produced the expected products, which were immunoprecipitated with a mouse monoclonal anti-HA antibody. Immunohistochemical studies with hepatocyte cell lines transiently transfected with either $mC3_{NLS}$ or $mC3_Y$ showed only cytoplasmic staining, whereas cells transfected with mC3 had a staining pattern typical of endogenous RRC3 (both cytoplasmic and nuclear) with strong staining of the nuclear perimeter. Immunoblot analyses of subcellular fractions from stably transfected CWSV1 cells showed mC3 product in both the cytosol and nucleus of cells, whereas $mC3_{NLS}$ or $mC3_Y$ products were restricted to the cytosol. CWSV1 cells stably transfected with the pTet-Splice vector containing no insert (as a control) were markedly inhibited (80%) in cell growth and showed altered morphology when treated with antisense oligonucleotides targeted to endogenous RRC3, reproducing previous studies. Similarly, CWSV1 cells stably transfected with either $mC3_{NLS}$ or $mC3_Y$ constructs showed analogous growth inhibition and morphologic alteration upon antisense treatment. In contrast, CWSV1 cells stably transfected with the mC3 construct showed normal growth and morphology following antisense oligonucleotide treatment, demonstrating that replenishment of nuclear RRC3 was necessary and sufficient to relieve growth inhibition. In ^{32}P-metabolic labeling studies, mC3 was tyrosine-phosphorylated in cytosol as the full-length protein (M_r 36 000). $mC3_{NLS}$ was also phosphorylated in cytosol, whereas $mC3_Y$ was not. Nuclear mC3 showed phosphorylation of a M_r 27 000 processed form while neither $mC3_{NLS}$ nor $mC3_Y$ showed any phosphorylated nuclear products. Our results show that nuclear RRC3 is important in control of cell growth and that both the NLS and Y_{121} are important in nuclear localization of RRC3. Control of nuclear import by tyrosine phosphorylation may represent a novel regulatory mechanism, and our results further suggest that RRC3 may travel as a maverick subunit.

Multicatalytic proteinases (MCPs)[1] are macromolecular complexes (M_r 2 × 10^6) which function as a major nonlysosomal pathway for protein degradation in cells (Peters *et al*., 1994). They are generally isolated as a large 26S complex from cytosol and are involved in the breakdown of abnormally folded proteins as well as in the breakdown of a multitude of regulatory proteins with very short half-lives (Hershko & Ciechanover, 1992; Hough *et al*., 1987). Degradation by the 26S MCP can be either ubiquitin-dependent or ubiquitin-independent and is both ATP-dependent (Hough *et al*., 1987; Tsukhara *et al.*, 1988) and Ca^{2+}-dependent (Dahlmann *et al*., 1989). Further purification of the 26S MCP results in the loss of these activities along with several associated regulatory complexes to yield

† This work was supported by grants from the National Institutes of Health (CA21141 and CA40145).

* Corresponding author. Mailing address: Department of Experimental Pathology, The Hershey Medical Center, P.O. Box 850, Hershey, PA 17033. Phone: (717) 531-5632. Fax: (717) 531-5298. Email: gac4@psu.edu.

⊗ Abstract published in *Advance ACS Abstracts,* August 15, 1996.

[1] Abbreviations: MCP, multicatalytic proteinase; NLS, nuclear localization signal; HA, hemagglutinin; EGF_R, epidermal growth factor receptor; I_R, insulin receptor; FGF_R, fibroblast growth factor receptor; NS, nuclear scaffold; PCR, polymerase chain reaction; CDM, chemically defined medium; HRP, horseradish peroxidase.

S0006-2960(96)00889-6 CCC: $12.00

a 20S particle believed to constitute the catalytic core of the MCP (Hoffman & Rechsteiner, 1994).

The structure of the 20S core particle is that of a barrel consisting of four rings, each ring containing seven subunits. Individual subunits (14 have been identified in human) of the 20S particle are of M_r 21 000−35 000 and are classified as α or β on the basis of homology to the prototypical MCP subunits from the archeabacterium *Thermoplasma acidophilium*, which has only one α and one β subunit (Puhler *et al*., 1992). The two outer rings of the 20S core contain α subunits, which are believed to be structural in nature, while the two inner rings contain β subunits, believed to form the catalytic center of the complex ($\alpha_7\beta_7\beta_7\alpha_7$; Puhler *et al*., 1992). In addition to archeabacteria, proteasomes of similar structure have also been identified in all eukaryotes examined and recently in eubacteria (Lupas *et al*., 1994; Tamura *et al*., 1995).

MCPs are characteristically found in both the cytoplasm and nucleus of cells (Tanaka *et al*., 1989; Rivett *et al*., 1992), although factors governing nuclear localization are not clear. While the functionality of the NLS from several human subunits has recently been documented (Nederlof *et al*., 1995), only four rat subunits, RRC3, RRC9, RRC6, and Iota (all α subunits), contain a putative NLS which may function in nuclear import. In addition to the NLS, the rat subunits RRC3 and RRC9 also have a potential site for tyrosine phosphorylation (Y_{121}) which shows homology to a number of tyrosine kinase autophosphorylation sites and which may also play a role in nuclear localization (Tanaka *et al*., 1990b).

We have previously demonstrated that whereas RRC3 is found in both the cytosol and nucleus of cells, only the nuclear form of RRC3 contains phosphotyrosine (Benedict *et al*., 1995), and we suggested that tyrosine phosphorylation triggered rapid nuclear import. The nuclear form of RRC3 was also implicated in cell growth (Benedict *et al*., 1995), since treatment of cells with an antisense oligonucleotide targeted to the translation initiation region of RRC3 inhibited cell growth by >90%. Under these treatment conditions RRC3 mRNA was no longer detectable, and RRC3 protein levels were dramatically reduced (>95%) in the nuclear scaffold (NS), whereas they showed only a moderate reduction in cytosol. Interestingly, nuclear MCP protease activity was not affected by modulation of RRC3 content.

To determine if the NLS and/or the potential tyrosine phosphorylation site (Y_{121}) is involved in nuclear localization of RRC3, we generated a variety of modified RRC3 expression constructs containing point mutations in either the putative NLS or Y_{121}. These constructs also contained an HA epitope tag and nucleotide alterations in their 5′ ends (a number of nucleotide alterations were introduced at "wobble" positions near the translation initiation site) which render them insensitive to the RRC3 antisense oligonucleotide treatment previously described (Benedict *et al*., 1995), yet will translate an identical RRC3 protein. Use of these constructs in transfection protocols indicates that both the putative NLS and Y_{121} are essential for nuclear localization of RRC3, suggesting a novel mechanism for control of nuclear import. Furthermore, treatment of hepatocyte cell lines with an antisense oligonucleotide targeted to the translation initiation sequence of RRC3, which selectively curtails expression of endogenous RRC3, was used to show that growth inhibition due to RRC3 depletion is selectively dependent upon loss of nuclear RRC3. As before, this growth inhibition was not reflective of any change in nuclear MCP proteolytic activity.

MATERIALS AND METHODS

Production of RRC3 Constructs. The polymerase chain reaction (PCR) was utilized to develop RRC3 constructs containing no mutations or point mutations either at the putative NLS ($KK_{51}QK$) or at a potential site of tyrosine phosphorylation (Y_{121}). 5′ and 3′ primers for control RRC3 were 5′AAGGAAAAAAGCGGCCGCGTAAAGATGGCAGAACGCGGT3′ and 5′CCGGAATTCCGCTATAGCAGCCAAGTAATC3′. For the construction of the NLS-mutated RRC3 construct, two sets of primers were utilized. The first set for the 5′ portion of the construct consisted of the 5′ RRC3 control primer and an internal 3′ primer containing a point mutation in the NLS (K_{51} mutated to A), 5′GGATTTCTGCGCTTTCTCAGTGGC3′. The second set for the 3′ portion of the construct contained the 3′ primer from control RRC3 and the internal primer 5′GCCACTGAGAAAGCGCAGAAATCT3′, which also contained the point mutation at K_{51} in the NLS. The two PCR fragments were ligated to form the complete mutant NLS construct. Constructs with mutations at the site of putative tyrosine phosphorylation (Y_{121} mutated to F) were made in the same manner; the internal 3′ and 5′ primers were 5′TGACTGGGTAAACTCTTGCATCAC3′ and 5′GTGATGCAAGAGTTTACCCAGTCA3′, respectively. An HA epitope (a gift from Dr. Anita Hopper) was then ligated in triplicate to the C-terminus of the constructs. The HA fragment was also generated by PCR with the 5′ primer 5′CCGGAATTCGGCCGCATCTTTTACCCATAC3′ and the 3′ primer 5′TTTTCCTTTTGCGGCCGCACTGAGCAGCGTAATCTGG3′. Control RRC3 constructs are designated C3 while constructs containing NLS or Y_{121} mutations are designated $C3_{NLS}$ and $C3_Y$, respectively.

These constructs were then modified in the nucleotide base composition at the translation initiation site of RRC3 by introducing nucleotide alterations in such a way that the amino acid sequence of the protein translated from the constructs would be identical to that of normal RRC3. The modified 5′ primer for these PCR amplifications was 5′AAGGAAAAAAGCGGCCGCGTAAAG**ATGGCCGAGAGGGGATATTCG**TTCTCGCTGACTACA3′ (the region targeted by antisense oligonucleotides is in bold, and modified nucleotides are underlined). These constructs thus differ in 9 of 21 nucleotides from endogenous RRC3, allowing differential inhibition by antisense oligonucleotide treatment (see below). The control RRC3 construct containing the N-terminal modifications is designated mC3, whereas the corresponding NLS and Y_{121} mutants are designated $mC3_{NLS}$ and $mC3_Y$, respectively.

Finally, RRC3 constructs were developed with missense mutations (M to L) at the translation initiation start site (M_1) and/or at an internal in-frame ATG (M_{79}) using a similar strategy. For amplification of the RRC3 constructs mutated at M_1 the 5′ primer 5′AAGGAAAAAAGCGGCCGCGTAAAGTTGGCAGAACGCGGT3′ was utilized, and for production of the RRC3 constructs mutated at M_{79} the internal 3′ and 5′ primers were 5′GTAATCTGGACCCAAGCCGCTGTACAC3′ and 5′GTGTACAGCGGCTTGGGTCCAGATTAC3′, respectively.

All RRC3 constructs described above were ligated into the pCRII vector (Invitrogen, San Diego, CA) and sequenced

in their entirety using universal M13 primers and several of the internal primers mentioned previously. After construction in the pCRII vector, all RRC3 constructs were also placed in a pOPRSVI CAT vector (Stratagene, La Jolla, CA) or a pTet-Splice vector (Gibco BRL, Gaithersburg, MD). For pOPRSVI CAT the sequences were removed from pCRII by digestion with *Not*I. The vector was also cut with *Not*I and the two were ligated using T4 DNA polymerase. [Orientation was verified by *Hin*dIII digestions (constructs in the correct orientation produced fragments of 381, 621, and 5078 bases), and identity of the inserts was again confirmed by DNA sequencing]. To place RRC3 constructs in the pTet-Splice vector the sequences were removed from pCRII by digestion with *Eco*RV and *Spe*I. The fragments were then ligated into pTet-Splice, which was also cut with these two enzymes, in an orientation-specific manner.

In Vitro Transcription/Translation. Promega's (Madison, WI) TNT-coupled reticulocyte lysate transcription/translation system was utilized with RRC3 constructs in the pCRII vector. Reactions were performed using T7 polymerase and [^{35}S]methionine (DuPont NEN, Boston, MA) for 90 min at 30 °C according to manufacturer's directions. An aliquot (5 μL) of product was separated by SDS−PAGE (Laemmli, 1970) on 12% gels at 40 mA for 4 h, and then soaked in EN^{3}HANCE (DuPont NEN) for 1 h and rinsed with water for 30 min. Gels were dried for 2 h and exposed to autoradiographic film at −70 °C. Typical exposures were 1−4 h.

Stability of RRC3 constructs was determined by incubation of 1 μL of each of the radioactively labeled transcription/translation products with 25 μg of cytosol (isolated as a 100000*g* supernate from a rat hepatocyte cell line) for 1, 4, 8, and 25 h at 37 °C. The proteins were then separated by SDS−PAGE, and gels were dried and exposed to autoradiographic film as described.

Anti-HA Immunoprecipitations. Polyclonal antiserum was raised in rabbits against a 10 amino acid peptide (CYPYDVPDYA) from influenza hemagglutinin. The peptide was coupled to keyhole limpet hemocyanin using the Imject Activated Immunogen Conjugation Kit (Pierce, Rockford, IL) and sent to Cocalico Biologicals (Reamstown, PA) for antiserum production. Two antiserum preperations were obtained and subsequently affinity purified using a column of HA peptide coupled to bovine serum albumin. An ImmunoPure Ag/Ab Immobilization Kit (Pierce) was used for column preparation. Affinity-purified antibodies were obtained from both antisera and gave results similar to those of dot blot analyses (each recognized 1 μg of HA peptide when used at a 1:1000 dilution). In some experiments, a mouse monoclonal anti-HA antibody (Boeinger Mannheim, Indianapolis, IN) was utilized.

Radioactively labeled products from transcription/translation reactions were immunoprecipitated using a mouse monoclonal anti-HA antibody (Boeinger Mannheim). Immunoprecipitations were done at 4 °C overnight and contained 10 μL of translation product and 2 μg of anti-HA antibody in a mixture of protease inhibitors (Tokes & Clawson, 1989), 0.1% SDS, and 50 mM ammonium sulfate and in a final volume of 1 mL with buffer A (500 mM HEPES, pH 7.9, 10% glycerol, 200 mM EDTA, 100 mM DTT; Kolodziej & Young, 1991). Protein A−Sepherose beads (Sigma, St. Louis, MO), preswollen in TENN (50 mM Tris, pH 7.4, 5 mM EDTA, 0.15 M NaCl, 0.5% NP40), were then used to bind precipitates at room temperature for 30 min. The beads were pelleted and washed twice with SNNTE (0.15 M sucrose, 0.5 M NaCl, 1% NP40, 50 mM Tris, pH 7.4, 5 mM EDTA) and once with RIPA (50 mM Tris, pH 7.4, 0.15 M NaCl, 1% Triton X-100, 0.1% SDS, 24 mM deoxycholic acid). Beads were boiled in SDS sample buffer, and the solubilized proteins were separated by SDS−PAGE. Gels were dried and exposed to autoradiographic film as previously described.

Transient Transfections and in Situ Localizations. For these studies CWSV1 cells, an SV40 immortalized rat hepatocyte cell line, and NR4 cells, a *ras*-transformed cell line derived from CWSV1 cells (Isom *et al*., 1992), were utilized. Cells were maintained in chemically defined medium (CDM) as previously described (Woodworth *et al*., 1986). NR4 or CWSV1 cells were plated on Falcon 3003 tissue culture dishes or on ProbeOn Plus microscope slides. After being seeded for 24 h, they were transfected with C3, $C3_{NLS}$, or $C3_Y$ RRC3 constructs contained in the pOPRSVI CAT vector using lipofectin (Gibco BRL) as a DNA carrier. Typical transfections contained lipofectin at a concentration of 40 μg/mL and 2 μg of DNA in a total volume of 4 mL of OPTI-MEM I media (Gibco BRL). Cells were treated at 37 °C for 4 h (Benedict *et al*., 1995) after which time the medium was changed to regular CDM. The cells were then allowed to grow for 24 h before being fixed with 4% paraformaldehyde in PBS (15 min) and permeabilized with 1% NP40 in PBS (20 min).

In situ localizations were performed as previously described (Benedict *et al*., 1995). Primary antibody, a mouse monoclonal anti-HA antibody, was used at a concentration of 3 μg/mL, and secondary antibody, a biotinylated rabbit anti-mouse antibody was used at a 1:400 dilution (Dako, Carpinteria, CA). Detection was as described using standard alkaline phosphatase procedures (Benedict *et al*., 1995).

Stable Transfections. CWSV1 cells were transfected with mC3, $mC3_{NLS}$, or $mC3_Y$ in the pTet-Splice vector. pTet-tTAk, which contains the gene for the tetracycline repressor (tTA), and pRSVneo, which contains the neomycin resistance gene, were cotransfected. Cells were treated when they were 80% confluent, and each lipofectin transfection contained 6 μg/mL pTet-Splice with insert, 2 μg/mL pTet-tTAk, and 2 μg/mL pRSVneo in a final volume of 2 mL OPTI-MEM I media for 4 h. The medium was then changed to CDM containing 1 or 5 μg/mL tetracycline. After 24 h transfected cells were selected by addition of G418 (Sigma) at a concentration of 500 μg/mL. Cell death of untransfected cells was apparent after 24 h, and the remaining cells were grown in media containing G418 and tetracycline. Uniform populations of G418-resistant cells were obtained after approximately 4 weeks of continuous selection (about four passages). Tetracycline was subsequently removed from various cell populations. CDM was changed every other day.

Western Blot Analysis. Ten 100 mm dishes of each of the stably transfected cell populations were used to prepare nuclear and cytosolic fractions. Cells (at approximately 1 $\times$ 10^7 cells/plate representing about 80% confluency) were homogenized in TKMC (50 mM Tris, pH 7.4, 25 mM KCl, 5 mM $MgCl_2$, 10 μM $CaCl_2$) and then centrifuged for 5 min at 6000*g*. The crude pellet was then rinsed in TKMC containing 1% Triton X100, and the nuclear pellet was obtained by centrifugation at 16000*g* for 20 min through a 1 M sucrose−TKM_2C cusion (sucrose of the specified

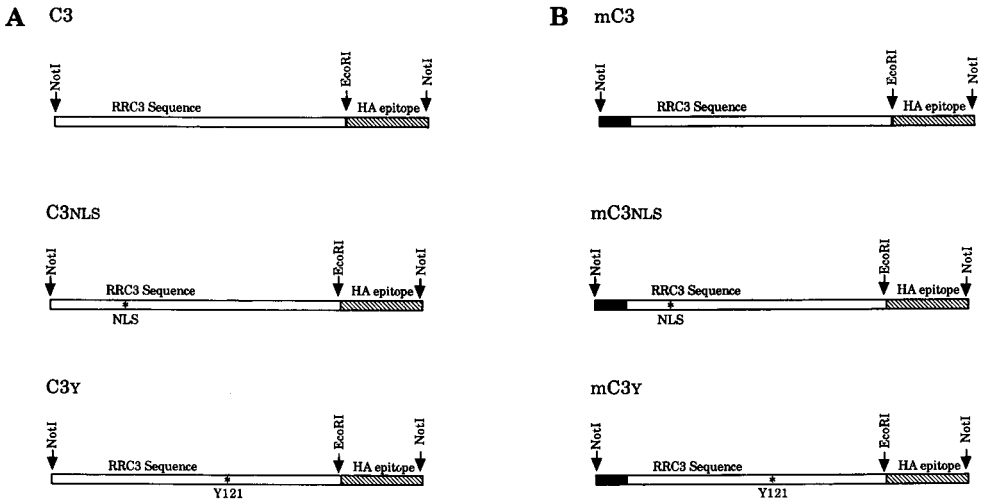

FIGURE 1: Schematic of RRC3 DNA constructs. (A) PCR was utilized to develop expression constructs which contain MCP subunit RRC3 in frame with an HA epitope (hashed boxes). The constructs shown are C3 (normal RRC3, top), $C3_{NLS}$ (RRC3 with a mutated NLS, middle), and $C3_Y$ (RRC3 with a mutated Y_{121}, bottom). Mutation sites are shown with an astrisk. (B) Additional mutant constructs were also developed in which the nucleotides of the translation start site of RRC3 have been modified in a number of codons at wobble positions (solid boxes). These modifications were made in such a way that the amino acid sequence of the protein translated from the constructs will be that of normal RRC3, in the context of a strong Kozak sequence. These constructs are designated mC3 (top), $mC3_{NLS}$ (middle), and $mC3_Y$ (bottom).

molarity, 50 mM Tris, pH 7.4, 25 mM KCl, 5 mM $MgCl_2$, 5 mM 2-mercaptoethanol, 10 μM $CaCl_2$). Cytosol was obtained as the supernate from a 100000*g* centrifugation. Nuclear and cytosolic proteins were separated by SDS−PAGE on 12% gels at 40 mA for 4 h. The proteins were transferred to Immobilon P PVDF membranes (Millipore, Bedford, MA), and immunodetection was performed as previously described (Benedict *et al*., 1995). Primary antibody was the mouse monoclonal anti-HA, used at a concentration of 5 μg/mL, and the secondary antibody was anti-mouse IgG $F(ab')_2$ fragments coupled to horseradish peroxidase (HRP), used at a 1:1000 dilution. Proteins were detected with ECL reagents (Amersham, Arlington Heights, IL) according to kit directions.

Metabolic [^{32}P]Orthophosphate Labeling and Anti-Phosphotyrosine Immunoprecipitations. For metabolic labeling studies, four 100 mm plates of CWSV1 cells (approximately 1×10^7 cells/plate) stably transfected with mC3, $mC3_{NLS}$, or $mC3_Y$ constructs were incubated with 300 μCi of [^{32}P]-orthophosphate (Amersham, specific activity 9000 Ci/mmol) in phosphate-free CDM containing G418. After 24 h, cells were rinsed with PBS and harvested by scraping, and nuclei and cytosol were prepared as described (Benedict *et al*., 1995), except that the homogenization buffer also contained vanadate at 1 mM. Nuclear and cytosolic fractions were used in immunoprecipitations with anti-HA antibodies (described above) and the precipitated proteins separated by SDS−PAGE. Gels were dried and exposed to autoradiographic film at −70 °C.

^{32}P-Labeled proteins were cut from dried gels, reconstituted in standard SDS−PAGE buffer, and electroeluted at 200 V for 2 h using a centrilutor micro-electroeluter (Amicon, Beverly, MA). Eluates were immunoprecipitated with 5 μg of anti-phosphotyrosine antibody (ICN Biomedicals, Costa Mesa, CA) at 4 °C overnight and immunoprecipitated as described above.

Antisense Oligonucleotide Studies. Antisense phosphorothioate oligonucleotides targeted to endogenous RRC3 were obtained from National Biosciences (Plymouth, MN) and have been described previously (Benedict *et al*., 1995). For these studies, the above mentioned stably transfected CWSV1 cells were plated at a density of 1×10^5 cells/60 mm dish in CDM containing G418 and tetracycline. The cells were grown for 24 h and then transfected with 0.2 μM antisense oligonucleotide with lipofectin for 4 h at 37 °C. After treatment, the cells were maintained for 4 days in either CDM containing G418 and tetracycline or CDM containing only G418. Cell growth was monitored with cell counts, and morphology was examined as described (Benedict *et al*., 1995).

Protease Activity Assays. Nuclear fractions were prepared from each of the stably transfected CWSV1 cell populations that had been treated with RRC3 antisense oligonucleotides or lipofectin only in the presence or absence of tetracycline as described. Protease activity of the fractions was assessed with the fluorescent chymotrypsin substrate $LLVY_{AMC}$ (Enzyme System Products, Dublin, CA) as previously described (Benedict *et al*., 1995). Each reaction contained 2.5 μg of nuclear protein, 50 μM $LLVY_{AMC}$ substrate, and 0.5 μg/μL poly(L-lysine) and were run for 2, 4, 8, and 20 h.

RESULTS

RRC3 constructs containing no mutation (C3), a mutation at Y_{121} ($C3_Y$), or a mutation in the NLS ($C3_{NLS}$) were developed by PCR, and an in-frame HA epitope was placed in triplicate at the C-terminus as a means of identification (Figure 1A). Additional constructs were then made by altering the nucleotide sequence in the translation start region of RRC3 in such a way that the constructs code for normal RRC3 protein yet show only 50% homology to RRC3 antisense oligonucleotides targeted to the endogenous RRC3. These N-terminally modified constructs are designated mC3, $mC3_Y$, and $mC3_{NLS}$ (Figure 1B). Each of the constructs was placed in the pCRII, pOPRSVI CAT, and pTet-Splice vectors, and each insert was sequenced in its entirety.

The RRC3 constructs in the pCRII vector, C3, $C3_Y$, and $C3_{NLS}$, as well as mC3, $mC3_{NLS}$, and $mC3_Y$, were utilized in *in vitro* transcription/translation reactions and were separated

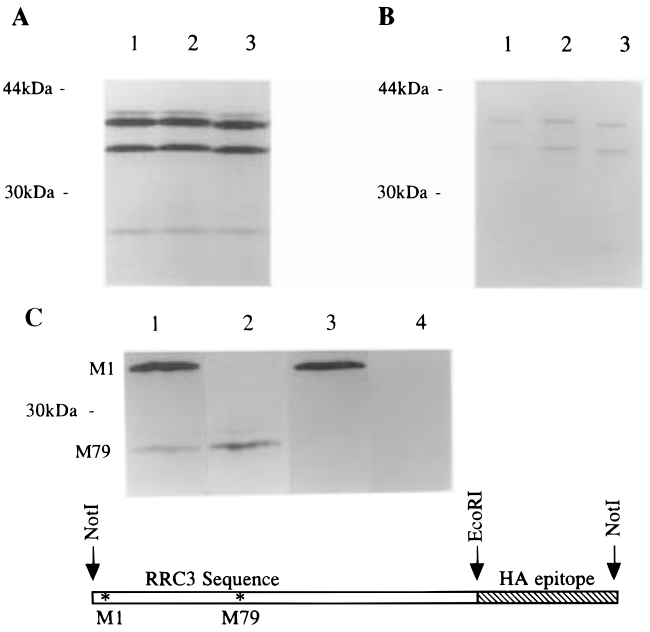

FIGURE 2: *In vitro* transcription/translation and immunoprecipitation of RRC3 constructs and mutational analysis of ATG codons in RRC3. (A) RRC3 DNA constructs in pCRII vector were utilized in *in vitro* transcription/translation reactions using a rabbit reticulocyte lysate system, T7 RNA polymerase, and [^{35}S]methionine. The products were separated by SDS−PAGE and visualized by autoradiography. Three proteins were produced from each of the constructs: the first from an in-frame ATG codon in the pCRII vector backbone (M_r 40 000), the second from the first ATG codon (M_1) in the RRC3 sequence (M_r 36 000), and the third from an internal in-frame ATG codon (M_{79}) in RRC3 (M_r 27 000). *In vitro* products from the RRC3 constructs C3, C3$_Y$, or C3$_{NLS}$ are shown in lanes 1, 2, and 3, respectively. (B) Products from *in vitro* transcription/translation reactions were immunoprecipitated with a mouse monoclonal antibody directed to the HA epitope. Precipitates were separated by SDS−PAGE and visualized by autoradiography. Proteins produced from both the vector and M_1 (M_r 40 000 and 36 000) were readily precipitated by the anti-HA antibody, comfirming that the RRC3 and HA sequences are in frame. The product from initiation at M_{79} (M_r 27 000) was also precipitated but was only apparent with longer autoradiographic exposures. Precipitated *in vitro* products from C3, C3$_Y$, or C3$_{NLS}$ DNA constructs are shown in lanes 1, 2, and 3, respectively. (C) RRC3 DNA constructs were developed with mutations at M_1 and/or M_{79}. Both ATG codons have strong Kozak sequences and serve as transcription initiation sites *in vitro*. The HA epitope is depicted as a hashed box, and sites of mutation are marked with an astrisk. *In vitro* transcription/translation reactions with the RRC3 construct C3 produced proteins of M_r 27 000 and M_r 36 000 (lane 1). Reactions with constructs mutated at M_1 eliminated production of the M_r 36 000 protein (lane 2), whereas reactions with constructs mutated at M_{79} eliminated production of the M_r 27 000 protein (lane 3). Constructs with both mutations (M_1 and M_{79}) produced neither the M_r 27 000 nor the M_r 36 000 (lane 4) protein. All constructs produced a M_r 40 000 (pCRII vector in-frame ATG) product (this band is not shown).

by SDS−PAGE. [^{35}S]Methionine-labeled products were then detected by autoradiography. Three major products with M_rs of 40 000, 36 000, and 27 000 were detected in reactions with each of the constructs (Figure 2A), and these products were all immunoprecipitated by a mouse monoclonal anti-HA antibody (Figure 2B). The origin of the three *in vitro* transcription/translation products was further examined with RRC3 constructs containing mutations in the proposed initiation start site ATG (M_1) and/or an internal ATG (M_{79}, Figure 2C). Both of these sites have consensus Kozak sequences (Kozak, 1989). *In vitro* transcription/translation reactions were run with the ATG mutant constructs, separated by SDS−PAGE, and visualized by autoradiography. A mutation at the initiation start site (M_1) of RRC3 eliminated the M_r 36 000 product (Figure 2C, lane 2), whereas a mutation at M_{79} prevented production of the M_r 27 000 product (Figure 2C, lane 3). Sequencing of the upstream pCRII vector revealed an in-frame ATG with a reasonable Kozak sequence (GTGATGG), translation from which produced the observed M_r 40 000 product: constructs containing both mutations produced neither the M_r 36 000 nor the M_r 27 000 products (Figure 2C, lane 4), although the M_r 40 000 protein was still produced in these reactions (data not shown).

Stability of the RRC3 construct products was also examined utilizing [^{35}S]methionine-labeled *in vitro* transcription/translation reactions. Reaction products were mixed with 25 μg of cytosol collected from CWSV1 cells and incubated at 37 °C for times up to 25 h. The proteins were then separated by SDS−PAGE and visualized by autoradiography. Products from all of the constructs were equally stable, showing little degradation even after extended (12−24 h) incubations with cytosol (data not shown).

To examine the role of the NLS or Y_{121} in nuclear localization of RRC3, the RRC3 constructs C3, C3$_{NLS}$, or C3$_Y$ were utilized in immunohistochemical analyses with NR4 and CWSV1 cells. NR4 and CWSV1 cells were transiently transfected with RRC3 constructs contained in the vector pOPRSVI CAT (without cotransfection of p3′SS, so that expression is induced) and subsequently stained 24 h later using an anti-HA antibody and standard alkaline phosphatase procedures (Figure 3). No significant staining was observed in the absence of primary antibody (Figure 3, panels A and E). In cells transfected with the C3 construct, a staining pattern similar to that seen for endogenous RRC3 was observed. Staining in these cells was both cytosolic and nuclear, with very strong staining of the nuclear perimeter (Figure 3, panels B and F). In NR4 and CWSV1 cells containing either C3$_{NLS}$ or C3$_Y$ constructs, however, only cytosolic staining was observed (Figure 3, panels D and H or C and G, respectively), suggesting that both the NLS and Y_{121} are important in nuclear localization.

To extend these results, stable CWSV1 transfectants were developed with mC3, mC3$_{NLS}$, or mC3$_Y$ constructs using the tetracycline inducible system (and pRSVneo vector to allow selection with G418). Nuclear and cytosolic fractions were collected from stably transfected CWSV1 cells and used for immunoblot analyses. RRC3 protein (M_r 36 000) was detected using anti-HA antibodies in both the cytosolic and total nuclear fractions from cells stably transfected with mC3 constructs (see Discussion). As was the case with endogenous RRC3, a relatively small percentage of total cellular mC3 was found in the nuclear fraction. RRC3 was only found in the cytosol of cells transfected with mC3$_{NLS}$ or mC3$_Y$ constructs using the anti-HA antibodies (Figure 4). These results confirm the immunohistochemical localizations.

[^{32}P]Orthophosphate metabolic labeling experiments were performed with CWSV1 cells stably transfected with mC3, mC3$_{NLS}$, or mC3$_Y$ constructs. Following labeling, cytosolic and total nuclear fractions were prepared in the presence of vanadate, a potent inhibitor of tyrosine phosphatases, and immunoprecipitations were performed with anti-HA antibody. CWSV1 cells stably transfected with mC3 contained full-length ^{32}P-mC3 protein (M_r 36 000) in the cytosol (Figure 5, lane 1), whereas they contained a processed form (M_r

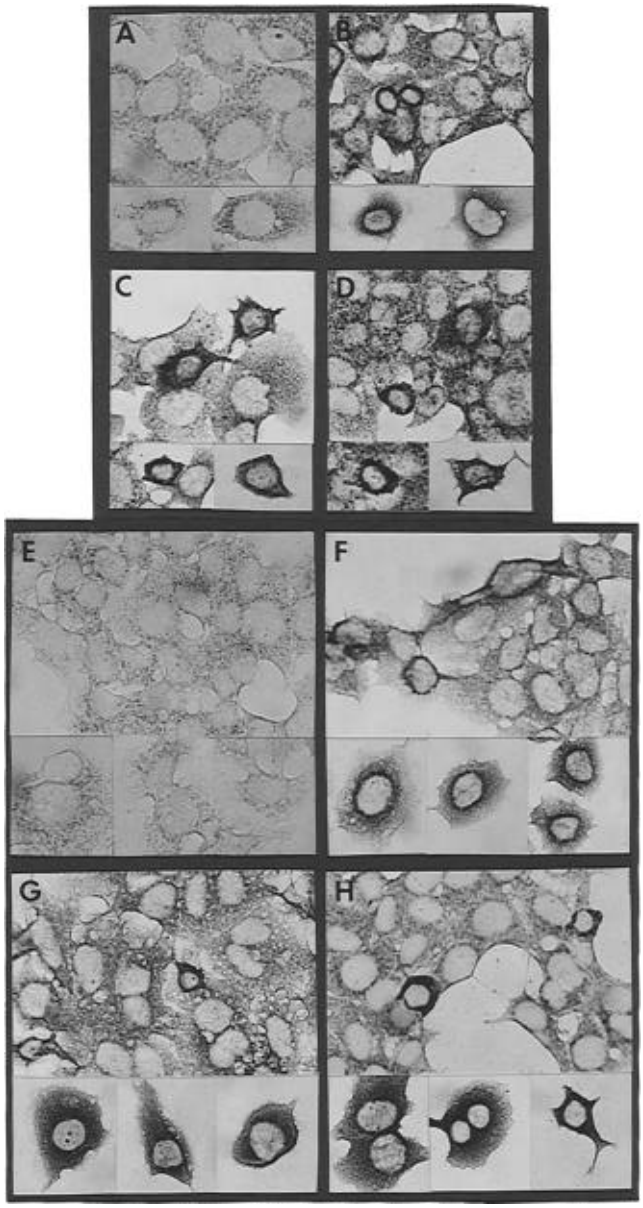

FIGURE 3: Immunohistochemistry of RRC3 DNA constructs in rat hepatocyte cell lines. NR4 (panels A−D) and CWSV1 (panels E−H) cells were transiently transfected with the RRC3 constructs C3, $C3_Y$, or $C3_{NLS}$ (or with no DNA) using lipofectin. Cells were maintained for 24 h in CDM and then stained with a mouse monoclonal anti-HA antibody and standard alkaline phosphatase immunohistochemical procedures. Panels A and E show background staining of NR4 and CWSV1 cells, respectively. Panels B and F (C3 construct) show staining of the nucleus and cytosol of cells, with predominant staining of the nuclear perimeter (a pattern typical for endogenous RRC3 localization), whereas panels C and G ($C3_Y$ mutant construct) or D and H ($C3_{NLS}$ mutant construct) show strong staining of only cytosol, indicating that nuclear localization of $C3_Y$ or $C3_{NLS}$ does not occur.

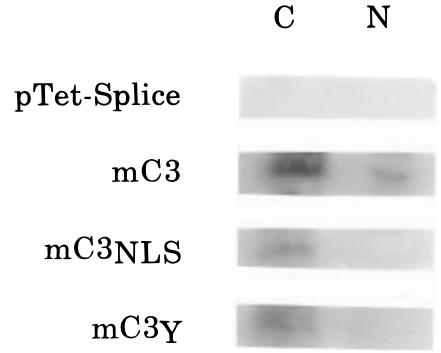

FIGURE 4: Subcellular localization of N-terminally modified RRC3 construct products. Cytosolic (C) and nuclear (N) fractions were prepared from CWSV1 cell populations stably transfected with the tetracycline-inducible system (cells contained pTet-tTAk, pRSVneo, and the pTet-Splice vector with mC3, $mC3_{NLS}$, $C3_Y$, or no insert). Proteins were separated by SDS−PAGE and transferred to Immobilon P membranes for immunoblot analysis with an anti-HA antibody. RRC3 protein produced from mC3 (M_r 36 000) was detected in both the cytosolic and nuclear fractions, whereas protein from $mC3_{NLS}$ or $mC3_Y$ constructs was detected only in the cytosolic fraction. No protein was detected in the cytosolic or nuclear fraction from cells containing the pTet-Splice vector without insert. Lanes contained 500 μg (mC3) or 200 μg ($mC3_{NLS}$ and $mC3_Y$) of cytosolic or nuclear proteins.

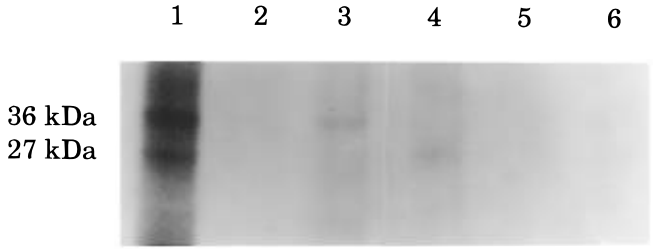

FIGURE 5: [^{32}P]orthophosphate labeling of N-terminally modified RRC3 constructs. Cytosolic and nuclear fractions were prepared from CWSV1 cell populations stably transfected with the RRC3 constructs mC3, $mC3_{NLS}$, or $C3_Y$, after metabolic labeling with [^{32}P]-orthophosphate. The fractions were immunoprecipitated with anti-HA antibodies, and the precipitates were subsequently separated by SDS−PAGE. Phosphorylated mC3 was observed in both the cytosol (as a full-length M_r 36 000 form, lane 1) and nucleus (as a processed M_r 27 000 form, lane 4) while ^{32}P-$mC3_{NLS}$ (M_r 36 000) was observed only in the cytosol (lane 3). Phosphorylated forms of $mC3_Y$ were not observed (lanes 2 and 5). Immunoprecipitations with mC3 cytosolic fractions were performed with 380 μg, whereas the other immunoprecipitations utilized 225 μg.

27 000) of ^{32}P-mC3 in total nuclear preparations (Figure 5, lane 4). This is analogous to previous results with RRC3 where a smaller processed form was specifically associated with NS (Benedict *et al.*, 1995). Documentation of the labeled M_r 36 000 found in the cytosol is probably attributable to use of the tyrosine phosphatase inhibitor during isolation (and to examination of more cytosolic protein). A minor quantity (about 10%) of the smaller M_r form was also observed in the cytosol, which we attribute to nuclear lysis during homogenization. CWSV1 cells transfected with $mC3_Y$ did not show any ^{32}P-labeled mC3 (Figure 5, lanes 2 and 5), while CWSV1 cells containing $mC3_{NLS}$ also contained full-length ^{32}P-mC3 in the cytosol (Figure 5, lane 3) but did not contain any ^{32}P-labeled mC3 in the nuclear fraction (Figure 5, lane 6). Precipitation of the ^{32}P-labeled proteins with an anti-phosphotyrosine antibody showed that all of the labeled proteins contained phosphotyrosine.

Previous results suggested that the nuclear form of RRC3 is selectively important in the regulation of cell growth: RRC3 antisense oligonucleotide treatment of CWSV1 or NR4 hepatocyte cell lines inhibited cell growth by 90% (Benedict *et al.*, 1995) while selectively depleting the nuclear form of RRC3. To extend these results, CWSV1 cells were stably transfected with the tetracycline-inducible constructs mC3, $mC3_{NLS}$, or $mC3_Y$ (or vector-only controls) and were subjected to the same RRC3 antisense oligonucleotide treatment protocol. This protocol allowed us to downregulate expression of endogenous RRC3 without effect on the expression of the transfected constructs. This was confirmed by Northern blot analyses (data not shown), which also

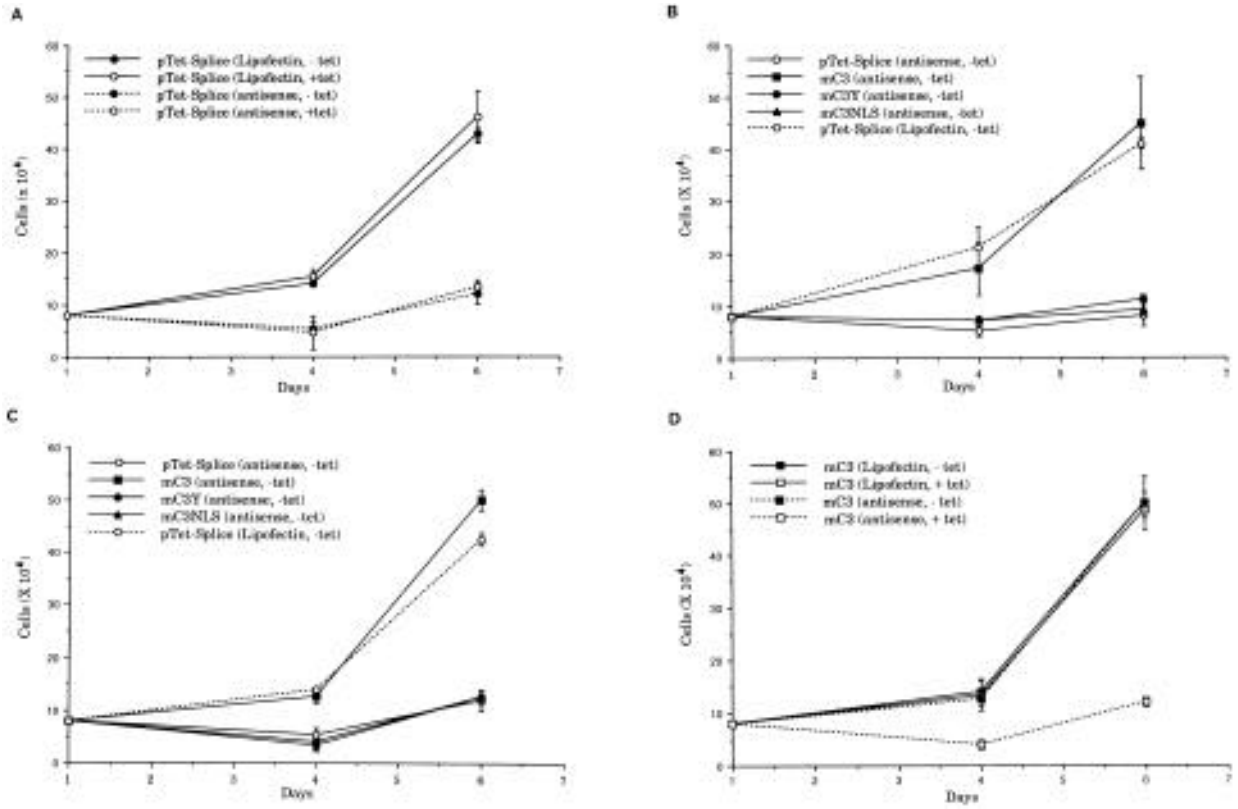

FIGURE 6: Antisense oligonucleotide treatment of CWSV1 cells stably transfected with N-terminally modified RRC3 constructs. CWSV1 cells were stably transfected with the pTet-Splice RRC3 constructs mC3, $mC3_{NLS}$, $mC3_Y$, or vector without insert and selected with G418. Populations of these cells were then treated with antisense oligonucleotides targeted to the translation initiation region of endogenous RRC3. Cells were maintained for 6 days, and cell counts were taken on days 3 and 6. Growth curves are shown for CWSV1 cells stably transfected with the following: panel A, pTet-Splice vector without insert and treated with lipofectin (+tet, ○, or −tet, ●; solid lines) or RRC3 antisense oligonucleotides (+tet, ○, or −tet ●; dashed lines); panels B and C (which depict results obtained in separate experiments), mC3 (−tet, ■), $mC3_{NLS}$ (−tet, ▲), $mC3_Y$ (−tet, ●), or pTet-Splice vector without insert (−tet, ○) and treated with RRC3 antisense oligonucleotides (solid lines) or lipofectin alone (dashed line); and panel D, mC3 and treated with lipofectin (+tet, □, or −tet, ■; solid lines) or RRC3 antisense oligonucleotides (+tet, □, or −tet ■; dashed lines).

showed that expression levels of the three constructs were equivalent. Following treatment, cells were maintained for 6 days and cell counts were taken on day 3 and day 6. At 6 days after treatment, growth of CWSV1 cells containing the pTet-Splice vector (with no insert) was dramatically inhibited under these conditions (>80%; Figure 6A), and the cells showed altered morphology (Figure 7B), reproducing our previous results (Benedict *et al*., 1995). In marked contrast, CWSV1 cells containing mC3 constructs and subjected to the antisense oligonulceotide treatment maintained a growth pattern similar to that of untreated cells (Figure 6, panels B and C) and showed normal morphology (Figure 7E). Further, relief from growth inhibition was completely dependent upon expression of mC3, as is evident from comparison of results with or without tetracycline (Figure 6D). CWSV1 cells stably transfected with either the $mC3_{NLS}$ or $mC3_Y$ constructs were unable to overcome the effects of antisense oligonucleotide treatment and remained growth inhibited even in the absence of tetracycline (78% and 73% at day 6, respectively; Figure 6, panels B and C), clearly establishing the functional importance of *nuclear* RRC3 in growth of this rat hepatocyte cell line. Cells containing $mC3_{NLS}$ or $mC3_Y$ also showed altered morphology (Figure 7, panels C and D), with tightly packed islands of cells reminiscent of earlier results with antisense oligonucleotide treated cells (Benedict *et al*., 1995).

To determine the effects of these treatments on nuclear protease activity, nuclear fractions were purified from the above mentioned stably transfected CWSV1 cells, with or without antisense oligonucleotide (or lipofectin) treatments, and tested for chymotrypsin-like activity with the fluorescent substrate $LLVY_{AMC}$. As was the case in studies on endogenous RRC3, nuclear protease activity was not significantly altered in any of the populations. In particular, in CWSV1 cells stably transfected with mC3, proteolytic activity was 1.3 versus 1.4 A_{460} flourescent units/(h·μg) in the presence or absence of tetracycline, respectively. Since these cell populations show dramatic differences in cell growth (Fig 6D), the results suggest that nuclear proteolytic activity is not directly related to growth inhibition or to nuclear RRC3 content (see Discussion).

DISCUSSION

Our results clearly establish the importance of nuclear RRC3 in cell growth control. RRC3 antisense oligonucleotide treatment results in a marked growth inhibition of rat hepatocytes, which encompasses loss of NS RRC3 with only modest effects on cytosolic RRC3. Here, using stably transfected cells expressing mC3, $mC3_{NLS}$, or $mC3_Y$ (in a tetracycline-dependent fashion), we show that this growth inhibition is alleviated only when nuclear RRC3 is replenished. That is, RRC3 proteins which are unable to enter the nucleus (from $C3_{NLS}$ or $C3_{Y)}$ do not overcome the growth inhibition by antisense oligonucleotide treatment which eliminates endogenous nuclear RRC3, whereas the mC3

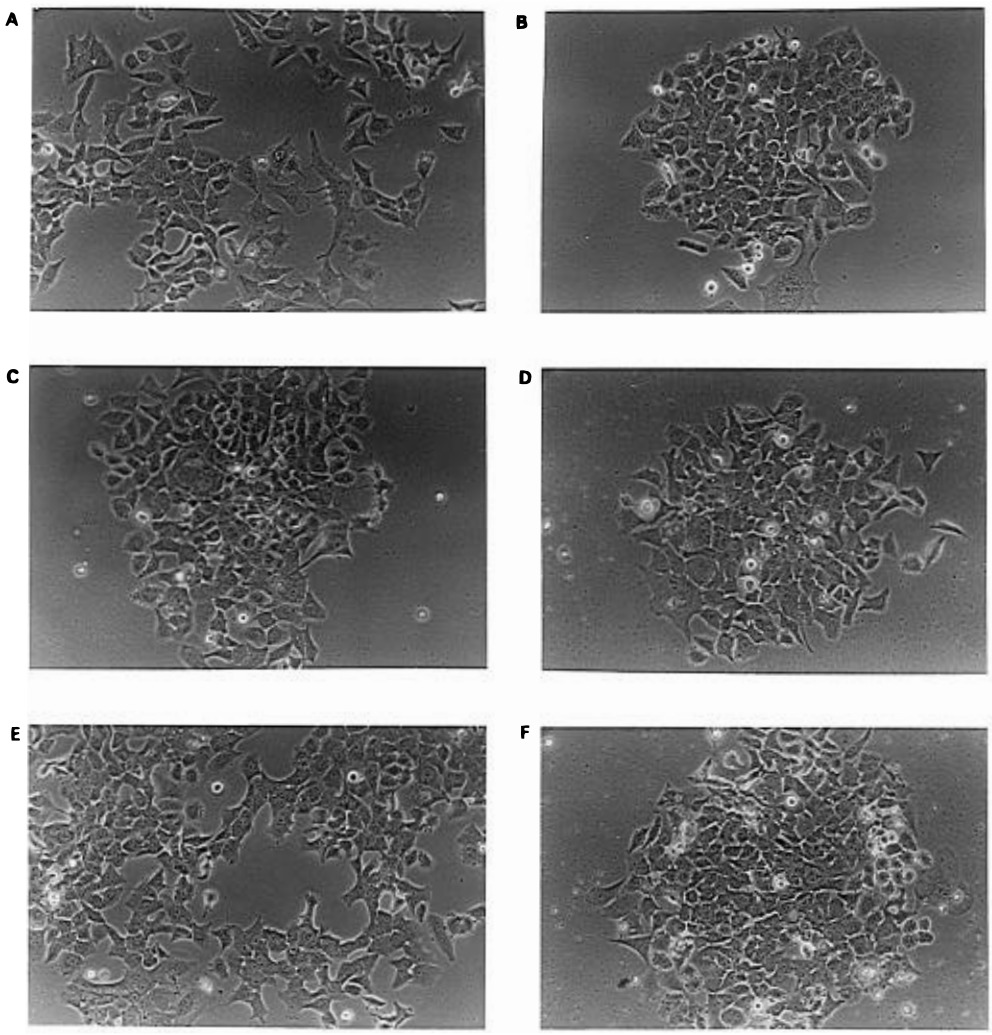

FIGURE 7: Effects of RRC3 antisense oligonucleotides and RRC3 constructs on the morphology of CWSV1 cells. Stably transfected CWSV1 cells (with mC3, mC3NLS, mC3Y, or pTet-Splice vector without insert) were treated with RRC3 antisense oligonucleotides or lipofectin only for 4 h. Cells were then maintained in the presence or absence of 5μg/mL tetracycline for 3 days and subsequently photographed using phase contrast microscopy. Representative photomicrographs show (A) cells transfected with pTet-Splice, treated with lipofectin only, and maintained in the absence of tetracycline (these cells show morphology typical of control CWSV1 cells); (B) cells transfected with pTet-Splice, treated with RRC3 antisense oligonucleotides, and maintained in the absence of tetracycline; (C) cells transfected with $mC3_{NLS}$, treated with RRC3 antisense oligonucleotides, and maintained in the absence of tetracycline; (D) cells transfected with $mC3_{Y}$, treated with RRC3 antisense oligonucleotides, and maintained in the absence of tetracycline. Cells in panels B, C, and D show significant growth inhibition and obtain a morphology of tightly packed clusters on otherwise sparsely populated plates, and panels E and F show cells transfected with mC3, treated with RRC3 antisense oligonucleotides, and maintained in the absence or presence of tetracycline (respectively). Expression of mC3 in the absence of tetracycline (panel E) restores normal growth, and the cells show normal morphology (see panel A). The presence of tetracycline (panel F) prevents expression of mC3 and prevents assumption of normal growth and morphology.

product does enter the nucleus and restores normal growth and morphology.

These results also clearly establish the importance of the NLS (KKQK) and Y_{121} in nuclear localization of RRC3. Recognition of the importance of the NLS confirms a recent report of Nederlof *et al*. (1995) regarding the functionality of the same NLS in the human C3 subunit. Demonstration of the involvement of Y_{121} in controlling nuclear import of RRC3 appears to define a novel mechanism for control of nuclear import, wherein tyrosine phosphorylation appears to trigger nuclear import of the target protein. Our results support a speculation made by Tanaka *et al.* (1990a), who noted some homology between the region of RRC3 surrounding Y_{121} and those surrounding tyrosine autophosphorylation sites in a number of growth receptors, including I_R and EGF_R. These receptors undergo autophosphorylation of the corresponding Y residue and presumably transduce signals on the basis of conformational changes induced by the phosphorylation. While standard searches with the RRC3 sequence (BLAST version 1.4, NCBI E-mail) did not identify I_R or EGF_R, the tyrosine autophosphorylation site of FGF_R was identified, which also showed conservation of numerous residues within the region noted previously.

In a previous study, tyrosine-phosphorylated RRC3 was found only in the nucleus, and a rapid downsizing occurred, so that nearly all phosphorylated RRC3 was smaller and specifically associated with the NS (Benedict *et al*., 1995). We proposed that RRC3 may be phosphorylated in the cytoplasm and that this phosphorylation is tightly coupled to nuclear import and subsequent proteolytic processing. This is now supported by the ^{32}P-metabolic labeling studies presented here, which differed from our previous studies in that isolations were performed in the presence of vanadate, a potent inhibitor of tyrosine phosphatases (and in that larger quantities of cytosolic protein were examined). This difference seems to indicate that tyrosine phosphatase activity

toward RRC3 is prevalent. Under these conditions, ^{32}P-mC3 protein was observed in cytosol as the expected M_r 36 000 form, and phosphorylation was observed not only with mC3 but also with $mC3_{NLS}$ transfectants. Further, ^{32}P-mC3 was quantitatively immunoprecipitated with antiphosphotyrosine antibodies. Nuclear ^{32}P-mC3 was significantly smaller (M_r 27 000) and was observed only with mC3, since $mC3_{NLS}$ and $mC3_Y$ were not present in the nucleus. The proteolytic processing (as with endogenous RRC3) must involve the N-terminus (given the C-terminal location of anti-RRC3 and anti-HA epitopes) and must occur very rapidly after nuclear import, since little or no unprocessed ^{32}P-mC3 was found in the rapidly isolated total nuclear fraction. We also noted a minor quantity (about 10%) of the M_r 27 000 ^{32}P-mC3 form in cytosol preparations, which we attribute to nuclear lysis during homogenization (since this also represents the typical distribution of DNA). We further note that the M_r 27 000 mC3 form generated by internal initiation at M79 would lack an NLS and that only a single RRC3 mRNA is present in Northern blot analysis.

On the basis of the crystallographic structure of the MCP from *T. acidophilium* (Lowe *et al*., 1995), the NLS is located near Y_{121} in three-dimensional structure. We therefore suggest that phosphorylation of Y_{121} may result in a comformational change which unmasks the NLS, triggering rapid import of endogenous RRC3 or mC3. FGF_R, EGF_R, and I_R may serve as paradigms for such a conformational change, based on homology to the region surrounding Y_{121}. We also note the presence of a short cluster of acidic amino acids E_{180}DLELED in RRC3, which could serve as a cNLS (Tanaka *et al*., 1990b) and which is predicted to be near the NLS in three-dimensional structure (Lowe *et al*., 1995). Phosphorylation of $mC3_{NLS}$ may likewise induce a conformational change, but the NLS is no longer functional and the protein therefore remains cytosolic.

Our results seem to imply the intriguing possibility that RRC3 may move to the nucleus and/or NS by itself, apart from MCP complexes which appear to contain several alternative functional NLS. Knuehl *et al*. (1996) found that mutation of the functional NLS in the subunit RRC6 (PROS 28.1) had little effect on its nuclear localization. In contrast, mutation of the NLS (or Y_{121}) in RRC3 completely abolished nuclear import. If RRC3 was similarly incorporated into MCP, one would clearly expect that some $mC3_{NLS}$ or $mC3_Y$ would be found in the nuclear fraction, which was not the case. By the same token, if MCP import was exclusively dependent upon RRC3, one would expect to see a decline in nuclear MCP content and/or activity following downregulation of RRC3, which again was not the case (although a long half-life could partially mask such effects).

We suggest the following model, in which RRC3 can be tyrosine-phosphorylated in the cytoplasm, which induces conformational changes and triggers its nuclear import (Figure 8). Once inside the nucleus, two alternative pathways are envisioned to exist. In one, dephosphorylation occurs, with subsequent incorporation into functional MCP found in the soluble nuclear fraction (Benedict *et al*., 1995). In the other pathway, proteolytic processing occurs, and the smaller M_r form of RRC3 (still containing phosphotyrosine) is tightly associated with the NS. Since tyrosine-phosphorylated RRC3 represents a minor fraction of total nuclear RRC3, this again seems to indicate that tyrosine phosphatase activity toward RRC3 is prevalent, since dephosphorylation

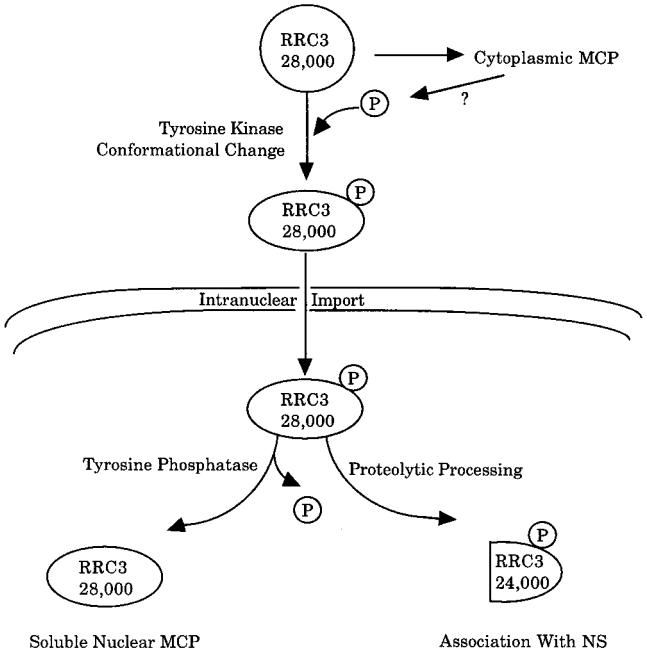

FIGURE 8: Proposed model for nuclear import of RRC3. In cytosol, RRC3 (M_r 28 000) may be incorporated into cytosolic MCPs in an unphosphorylated form or may alternatively be phosphorylated and subsequently targeted for nuclear import. Tyrosine phosphorylation (by an unidentified cytosolic tyrosine kinase) is envisioned to induce a conformational change in RRC3, which unmasks the NLS, thus triggering nuclear import. Our data are consistent with RRC3 trafficking as an individual subunit. Following import, RRC3 (M_r 28 000 for the endogenous form) can be proteolytically processed N-terminally to an M_r 24 000 form that becomes tightly associated with the NS, where it retains its phosphorylated tyrosine. Alternatively, unprocessed RRC3 (M_r 28 000) can also be dephosphorylated (by an unidentified nuclear tyrosine phosphatase), where it is incorporated into soluble nuclear MCPs. This latter pathway appears to predominate, since most nuclear RRC3 is not phosphorylated.

must represent the predominant pathway. We also speculate that incorporation of RRC3 into MCP may depend upon the N-terminal domain conserved among α subunits (Kloetzel *et al*., 1991), in which case the processed form of RRC3 would not associate with MCP complexes.

While endogenous RRC3 (which is actually present as three major isoforms at M_r 28 000, none of which is phosphorylated) is present in MCP in the soluble nuclear fraction, there is no clear evidence to suggest that RRC3 is contained within MCP after its proteolytic processing (conditions necessary to solubilize NS preparations destroy MCP structure). In fact, this proteolytic processing most likely dissociates RRC3 from the MCP structure, on the basis of a number of considerations. First, a number of MCP subunits prevalent in soluble nuclear MCP are absent in NS preparations (L. Ren and G. A. Clawson, manuscript submitted). Second, protease assays demonstrate that the NS content of RRC3 bears no relationship to nuclear or NS MCP proteolytic activity, either to total activity (Benedict *et al*., 1995) or specifically with regard to chymotrypsin-like activity [see Results and Benedict *et al*. (1995)] which is the predominant activity in soluble nuclear MCP and NS. These results raise the interesting possibility that the NS-associated RRC3 may somehow function independently from MCP. Regarding potential alternative functions for NS-associated RRC3, it is of some interest that the region surrounding Y_{121} also shows some homology to an OCS DNA binding protein in plants (Singh *et al*., 1990) and to an ATP-dependent RNA

helicase (Wilson *et al.*, 1994).

Although further work is necessary, our results suggest that the NS form of RRC3, alone or possibly in conjunction with RRC3 found in soluble nuclear MCP, is important in growth regulation.

ACKNOWLEDGMENT

We thank Dr. Harriet Isom for generously providing NR4 and CWSV1 cells and Dr. Anita Hopper for her gift of the influenza hemagglutinin epitope.

REFERENCES

Benedict, C. M., Ren, L., & Clawson, G. A. (1995) *Biochemistry 34*, 9587.

Dahlmann, B., Kopp, F., Kuehn, L., Neidel, B., Pfeifer, G., Hegerl, R., & Baumeister, W. (1989) *FEBS Lett. 251*, 125.

Hershko, A., & Ciechanover, A. (1992) *Annu. Rev. Biochem. 61*, 761.

Hoffman, L., & Rechsteiner, M. (1994) *J. Biol. Chem. 269*, 16890.

Hough, R., Pratt, G., & Rechsteiner, M. (1987) *J. Biol. Chem. 262*, 8303.

Isom, H., Woodworth, C., Meng, Y., Kreider, J., Miller, T., & Mengel, L. (1992) *Cancer Res. 52*, 940.

Kloetzel, P.-M., Frentzel, S., Gernold, M., Haass, C., Klein, U., Pesold-Hurt, B., & Seelig, A. (1991) *Biomed. Biochim. Acta 50*, 451.

Knuehl, C., Seelig, A., Brecht, B., Henklein, P., & Klotzel, P.-M. (1996) *Exp. Cell Res. 225*, 67.

Kolodziej, P. A., & Young, R. A. (1991) *Methods Enzymol. 194*, 508.

Kozak, M. (1989) *J. Cell Biol. 108*, 229.

Laemmli, U. (1970) *Nature 227*, 680.

Lowe, J., Stock, D., Jap, B., Zwickl, P., Baumeister, W., & Huber, R. (1995) *Science 268*, 533.

Lupas, A., & Zwickl, P. (1994) *Trends Biochem. Sci. 19*, 533.

Nederlof, P. M., Wang, H.-R., & Baumeister, W. (1995) *Proc. Natl. Acad. Sci. U.S.A. 92*, 12060.

Peters, J. M., Franke, W. W., & Kleinschmidt, J. A. (1994) *J. Biol. Chem. 269*, 7709.

Puhler, G., Weinkauf, S., Bachmann, L., Muller, S., Engel, A., Hegerl, R., & Baumeister, W. (1992) *EMBO J. 11*, 1607.

Rivett, A. J., Palmer, A., & Knecht, E. (1992) *J. Histochem. Cytochem. 40*, 1165.

Singh, K., Dennis, E. S., Ellis, J. G., Llewellyn, D. J., Tokuhisa, J. G., Wahleithner, J. A., & Peacock, W. J. (1990) *Plant Cell 2*, 891.

Tamura, T., Nagy, I., Lupas, A., Lottspeich, F., Cejka, Z., Schoofs, G., Tanaka, K., DeMot, R., & Baumeister, W. (1995) *Curr. Biol. 5*, 766.

Tanaka, K., & Ichihara, A. (1989) *Biochem. Biophys. Res. Commun. 159*, 1309.

Tanaka, K., Fujiwara, T., Kumatori, A., Shin, S., Yoshimura, T., Ichihara, A., Tonkunaga, F., Aruga, R., Iwqanaga, S., Kakizoka, A., & Nakanishi, S. (1990a) *Biochemistry 29*, 3777.

Tanaka, K., Yoshimura, T., Fujiwara, T., Kumatori, A., & Ichihara, A. (1990b) *FEBS Lett. 271*, 41.

Tokes, Z., & Clawson, G. (1989) *J. Biol. Chem. 264*, 15059.

Tsukhara, T., Ishiura, S., & Sugita, H. (1988) *Eur. J. Biochem. 177*, 261.

Wilson, R., Ainscough, R., Anderson, K., Baynes, C., Berks, M., Bonfield, J., Burton, J., Connell, M., Copsey, T., Cooper, J., Coulson, A., Craxton, M., Dear, S., Du, Z., Durbin, R., Favello, A., Fraser, A., Fulton, L., Gardner, A., Green, P., Hawkins, T., Hillier, L., Jier, M., Jonston, L., Jones, M., Kershaw, J., Kirsten, J., Laisster, N., Latreille, P., Lightning, J., Lloyd, C., Mortimore, B., O'Callaghan, M., Parsons, J., Percy, C., Rifken, L., Roopra, A., Saunders, D., Shownkeen, R., Sims, M., Smaldon, N., Smith, A., Smith, M., Sonnhammer, E., Staden, R., Sulston, J., Thierry-Mieg, J., Thomas, K., Vaudin, M., Vaughan, K., Waterson, R., Watson, A. Weinstock, L. Wilkinson-Sproat, J., & Wohldman, P. (1994) *Nature 368*, 32.

Woodworth, C., Secott, T., & Isom, H. (1986) *Cancer Res. 46*, 4018.

BI960889P